

PAPER • OPEN ACCESS

## Spectrum evolution of magnetostatic waves excited through ultrafast laser-induced heating

To cite this article: Ia A Filatov *et al* 2020 *J. Phys.: Conf. Ser.* **1697** 012193

View the [article online](#) for updates and enhancements.

You may also like

- [Magnetostatic interaction between two bubble skyrmions](#)  
M A Castro, D Mancilla-Almonacid, J A Valdivia *et al.*
- [Nonequivalence of the magnetostatic potential energy corresponding to the Ampère and Grassmann current element force formulas](#)  
Timothy M Minter
- [Hybrid quantum systems based on magnonics](#)  
Dany Lachance-Quirion, Yutaka Tabuchi, Arnaud Glippe *et al.*



**ECS**  
The  
Electrochemical  
Society  
Advancing solid state &  
electrochemical science & technology

**DISCOVER**  
how sustainability  
intersects with  
electrochemistry & solid  
state science research

# Spectrum evolution of magnetostatic waves excited through ultrafast laser-induced heating

Ia A Filatov<sup>1,2</sup>, P I Gerevenkov<sup>1</sup>, M Wang<sup>3</sup>, A W Rushforth<sup>3</sup>,  
A M Kalashnikova<sup>1</sup>, and N E Khokhlov<sup>1</sup>

<sup>1</sup>Ioffe Institute, 26 Politekhnicheskaya st., St. Petersburg, Russian Federation, 194021

<sup>2</sup>ITMO University, St. Petersburg, Russian Federation, 197101

<sup>3</sup>School of Physics and Astronomy, The University of Nottingham, NG7 2RD Nottingham, UK

E-mail: yaroslav.filatov@metalab.ifmo.ru

**Abstract.** We study experimentally the influence of the laser-induced temperature gradient on the parameters of propagating magnetostatic surface waves in thin film of the ferromagnetic metallic alloy Gallenol  $\text{Fe}_{0.81}\text{Ga}_{0.19}$ . The material has a pronounced magnetocrystalline anisotropy and exhibits the long-distance propagation of magnetostatic surface waves excited with femtosecond laser pulses. The excitation pulse heats up the sample locally, what leads to the spatial-temporal change of magnetization and anisotropy parameters of the film, and thus excites the magnetostatic surface waves. We show experimentally that the spectrum of the excited waves narrows as they propagate in such a gradient medium. By changing the orientation of external magnetic field with respect to anisotropy axes of the sample, we control whether the low- or high-frequency part of the spin waves spectrum is suppressed.

## 1. Introduction

In the modern world, the improving the methods of data transfer and processing is widely discussed. This fuels rapid development of alternatives to conventional electronics, such as photonics [1], straintronics [2], spintronics [3, 4], magnonics [5], etc. Magnonics explores physical processes associated with the spin-wave propagation in complex magnetic structures. Advantages of waves-based logic realized in magnonics could be implemented, for example, in image and speech recognition [6]. Actual tasks of magnonics-based technologies require efficient control of spin waves at sub-micron space and sub-picosecond time scales. Thus, the approaches of femtomagnetism [7, 8, 9] should be exploited in magnonics for the spin-wave propagation control, especially since the optical excitation of spin waves is demonstrated recently [10, 11].

In the present work we study experimentally the influence of ultrafast laser-induced heating on propagation of magnetostatic surface waves (MSSW) in a film of the ferromagnetic metallic alloy Gallenol  $\text{Fe}_{0.81}\text{Ga}_{0.19}$  (FeGa). Particularly, we show the narrowing of the spectrum of the laser-excited waves as they propagate away from the excitation spot. We suggest that this effect originates from the spatial gradient of magnetic parameters of the film induced by the laser pulse. Moreover, by changing the orientation of external magnetic field with respect to anisotropy axes of the sample, we control whether the low- or high-frequency part of the spin waves spectrum is suppressed.



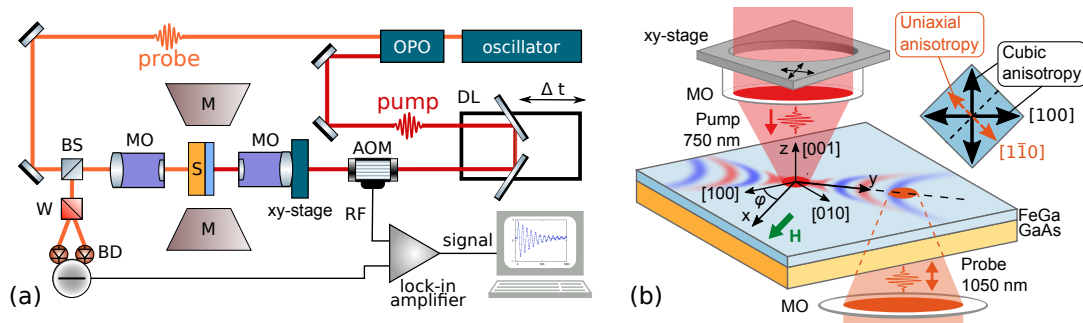


**Figure 1.** (a) Experimental setup: oscillator – Yb-doped solid-state oscillator laser system, OPO – optical parametric oscillator, BS – beam splitter, M – electromagnet, S – sample, MO – microobjective lens, DL – delay line, W – Wollaston prism, BD – balanced photodetector, AOM – acousto-optical modulator. (b) Geometry of the experiment.  $\mathbf{H}$  – external magnetic field applied along the  $x$ -axis of the laboratory frame;  $\varphi$  – the azimuthal angle between the  $x$ -axis and  $[100]$  crystallographic axis of the sample. The relative pump-probe distance is changed along the  $y$ -direction to detect propagation of MSSW. The blue-red pattern schematically represents MSSW propagation in the  $xy$ -plane. The inset shows the orientation of the easy magnetization axes of magnetocrystalline cubic (black) and growth-induced uniaxial (orange) anisotropy in the film plane.

## 2. Experiment

For our study, we chose a 20-nm thick film of a ferromagnetic metal Galfenol  $\text{Fe}_{0.81}\text{Ga}_{0.19}$  epitaxially grown on 530- $\mu\text{m}$  thick (001)-GaAs substrate. Epitaxial Galfenol films are characterized by a narrow ferromagnetic resonance [12], and large propagation length of MSSW [13]. The feature of the Galfenol films is pronounced magnetocrystalline cubic and growth-induced uniaxial anisotropy (see inset in Fig. 1(b)). The latter is associated with the FeGa/GaAs interface [12, 14].

Experiments are performed using all-optical pump-probe technique with spatial and temporal resolutions. Scheme of the setup and geometry of the experiments are shown in Figs. 1(a) and (b), respectively. The sample is placed in a magnetic field of  $H = 100$  mT applied in the plane of the film. The pump and probe 120-fs laser pulses with central wavelengths of 750 and 1050 nm, respectively, are focused on the sample with microobjective lenses (MO) into spots of 3  $\mu\text{m}$  in diameter. The pump-induced dynamics of an out-of-plane component of the film magnetization  $M_z$  is detected by measuring the polar magneto-optical Kerr rotation  $\Delta\theta_K$  for the probe pulse using an optical bridge detector composed of a Wollaston prism and a balanced photodetector.  $\Delta\theta_K$  is measured as a function of the time delay  $\Delta t$  between the pump and probe pulses. To detect the propagating laser-induced MSSWs, spatial scans  $\Delta\theta_K(\Delta y)$  are carried out by moving the probe MO with a piezoelectric  $xy$ -stage, thus changing the pump-probe distance along the  $y$ -axis, i.e. perpendicular to  $\mathbf{H}$ . Pump fluence is of 15  $\text{J}/\text{m}^2$ ; probe fluence is about 20 times lower. The measurements are performed at different angles  $\varphi$  between the crystallographic  $[100]$ -axis of the sample and the external magnetic field  $\mathbf{H}$ . All measurement are performed at room temperature.

## 3. Results and discussion

Figure 2(a) shows the temporal signals  $\Delta\theta_K(\Delta t)$  obtained at various pump-probe distances  $\Delta y$ , at  $\varphi = 45^\circ$  and  $\Delta x = 0$ , i.e. when the pump-probe distance  $\Delta y$  is scanned transversely to  $\mathbf{H}$ , corresponding to the MSSW configuration [15, 16]. Clear wave packets are seen in the signals, with amplitude decaying with  $\Delta y$ . The wave packet maximum shifts toward larger time

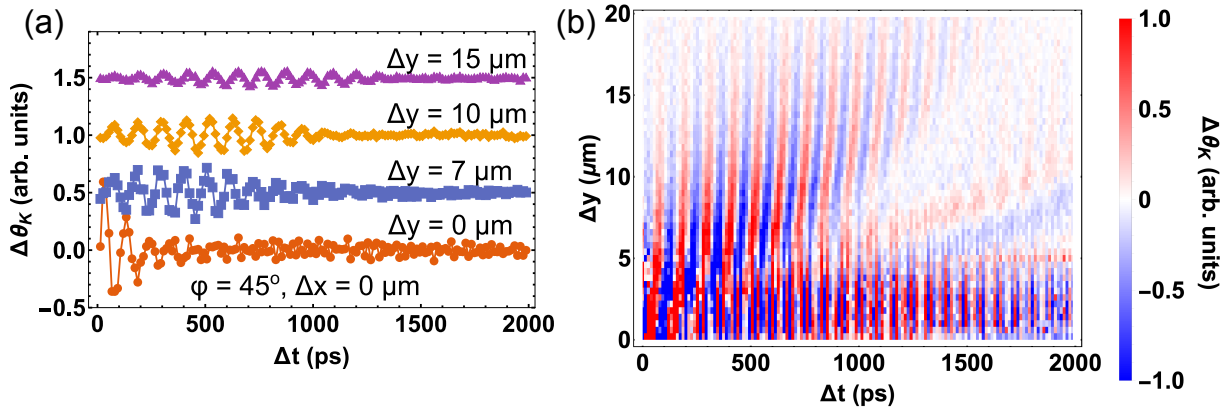


**Figure 2.** (a) Experimental temporal evolution of Kerr rotation  $\Delta\theta_K(\Delta t)$  at different pump-probe distances  $\Delta y$ , at  $\varphi = 45^\circ$  and  $\Delta x = 0$ . (b) Corresponding spatial-temporal  $\Delta y - \Delta t$  map of Kerr rotation  $\Delta\theta_K$  demonstrating the MSSW wave packet propagation.

delays  $\Delta t$  with  $\Delta y$ . It is even more evident on a spatial-temporal map  $\Delta y - \Delta t$ , shown on Fig. 2(b). Thus, the propagation of optically excited MSSW wave packet is registered in our experiments. The excitation mechanism of MSSW is an ultrafast change of the parameters of magnetic anisotropy due to the pump-induced heating, discussed in details in [13].

The variation of wave packet's amplitude with increase of the pump-probe distance  $\Delta y$  is determined by the Gilbert damping of Galfenol and the wave packet velocity, as discussed in [13, 17]. Therefore, here we focus our discussion on other important parameter of the wave packet – its spectrum. To explore the evolution of the MSSW's spectrum as a function of the pump-probe distance  $\Delta y$ , we have performed fast Fourier transform (FFT) of  $\theta_K(t)$  time-traces measured at different  $\Delta y$ . The results are shown in Fig.3 for two orientations of the external magnetic field,  $\varphi = 45^\circ$  and  $\varphi = 15^\circ$ .

The prominent change of the MSSW spectrum with increase of the pump-probe distance is evident in both geometries. The spectral width of the MSSW wave packet is decreasing as it propagates further from the excitation area. The change of the angle  $\varphi$  affects the character of the spectrum variation. Particularly, if  $\mathbf{H}$  is oriented closer to the hard magnetization axis of the sample ( $\varphi = 45^\circ$ ), the spectrum of the wave packet far outside of the pump spot is shifted towards the lower-frequency part of the MSSW spectrum seen within the pump spot (compare, e.g. spectra at  $\Delta y = 20 \mu\text{m}$  and  $\Delta y = 0$  in Fig. 3(a)). When  $\mathbf{H}$  is oriented closer to the easy magnetization axis of the sample, spectrum of the packet outside the pump spot is shifted towards the higher-frequency part of the spectrum observed within the pump spot ( $\Delta y = 10 \mu\text{m}$  and  $\Delta y = 0$  in Fig.3(b)).

The observed evolution of the MSSW wave packet spectrum can be explained by the spatial gradient of the magnetic anisotropy and magnetization in the Galfenol film emerging due to the laser-induced heating. Specifically, the femtosecond pump pulse abruptly increases the temperature of the sample, which is followed by cooling down taking much longer time of order of nano- and microseconds. It leads to the ultrafast decrease of the magnetization and magnetic anisotropy parameters within the area excited by the pump pulse [7, 9, 13]. These processes trigger the magnetization precession within this area and corresponding MSSW propagation with wavevectors in a range of  $0 \dots k_\sigma$ , where  $k_\sigma$  is limited by the pump spot size [13]. As the waves propagate up to  $10 \mu\text{m}$  and more, they inevitably pass through the material region with gradual changes of magnetic parameters. It makes the dispersion of MSSW variable along the packet propagation, and the character of variation is defined by the  $\varphi$ . Figures 3(c,d) illustrate schematically the limiting cases of the MSSW dispersion relation at  $\Delta y=0$ , i.e. in the center of

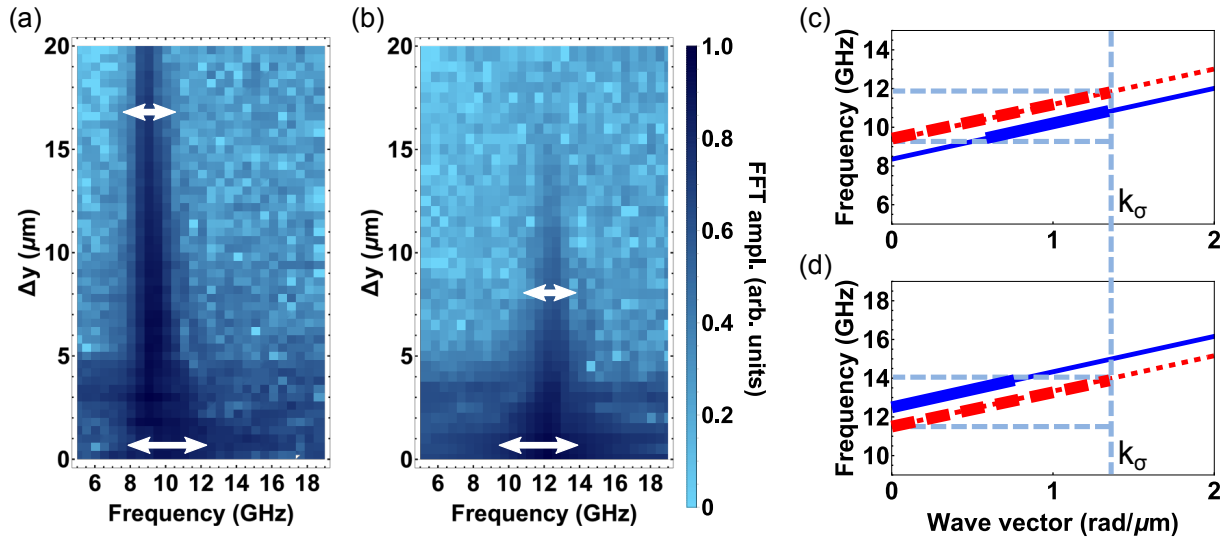


**Figure 3.** (a,b) FFT spectra of the MSSW packets at different pump-probe distances  $\Delta y$  at (a)  $\varphi = 45^\circ$  and (b)  $\varphi = 15^\circ$ . Arrows are guides to the eye showing the width of the spectra at different  $\Delta y$ . (c,d) Schematic representation of the MSSW dispersion  $f(k)$  changes when  $\mathbf{H}$  is along (c) hard and (d) easy anisotropy axes. Solid lines are the dispersions for a non-heated film; dashed red lines – dispersions for a heated film. Thicker segments show the range of MSSW frequencies and wavevectors which can be excited (red segments) and further propagate (blue segments). Vertical dashed lines represent limiting wave number  $k_\sigma$ .

the excited area, and at large  $\Delta y$ , at which the magnetic parameters of the film are those of the not-excited film. In particular, in the hard-axis configuration ( $\mathbf{H}$  is parallel to hard axis) the laser-induced ultrafast heating partly suppresses the effective anisotropy field  $H_a$  resulting in shift of the MSSW dispersion curve towards higher frequencies, as schematically illustrated in Fig. 3(c). The opposite situation takes place in the easy-axis configuration (see Fig. 3(d)). Taking into account that the range of the excited MSSW wavevectors is limited by  $k_\sigma$  (see red thick segments in Figs. 3(c,d)), it is easy to see that the MSSW spectrum far from the excitation area narrows and its central frequency shifts to higher or lower frequency depending on the field orientation (blue thick segments in Figs. 3(c,d)).

We note that the similar spectral changes were reported in [18] for Permalloy films. The distinctive feature of our experiments is in the presence of strong in-plane magnetic anisotropy providing the control of character of the changes – either to high or to low frequencies by in-plane rotation of the external field.

#### 4. Conclusions

In conclusion, we demonstrate the narrowing of the laser-induced magnetostatic surface waves spectra when the waves propagate in anisotropic Galfenol film. This narrowing results from the spatial gradient of magnetic parameters of the film induced by the same laser pulse as the one triggering the waves. The pronounced in-plane magnetocrystalline anisotropy provides an additional degree of freedom in tuning the character of the spectra changes, which is not feasible for in-plane isotropic films such as Permalloy. It should be noted that the laser-induced local change of the magnetostatic waves dispersion can lead to the formation of a potential well for MSSW, as demonstrated in Ref. [19]. Our investigation of the control of the character of the changes opens up new perspectives for the design of such MSSW traps in anisotropic materials. Furthermore, the concept of optically reconfigurable magnonic materials was demonstrated

recently using CW laser irradiation of a magnetic medium [20]. The ultrafast laser-induced changes of MSSW spectra demonstrated here open the new prospects for increasing operation rates of optically reconfigurable magnonic devices.

### Acknowledgments

Ia.A.F., P.I.G., and N.E.Kh thank RFBR (project № 20-32-70149) for support of the experimental part of study. N.E.Kh. thanks the Foundation for the Advancement of Theoretical Physics and Mathematics “BASIS” and the Russian Ministry of Education and Science (Megagrant project №075-15-2019-1934).

### References

- [1] Glick M, Kimmerling L C and Pfahl R C 2018 *Opt. Photon. News* **29** 36–41
- [2] Bukharaev A A, Zvezdin A K, Pyatakov A P and Fetisov Y K 2018 *Phys. Usp.* **61** 1175–1212
- [3] Hirohata A, Yamada K, Nakatani Y, Prejbeanu L, Diény B, Pirro P and Hillebrands B 2020 *Journal of Magnetism and Magnetic Materials* 166711
- [4] El-Ghazaly A, Gorchon J, Wilson R B, Patabi A and Bokor J 2020 *Journal of Magnetism and Magnetic Materials* **502** 166478
- [5] Nikitov S A *et al.* 2015 *Phys. Usp.* **58** 1002–1028
- [6] Albisetti E *et al.* 2020 *Advanced Materials* **32** 2070063
- [7] Kirilyuk A, Kimel A V and Rasing T 2010 *Rev. Mod. Phys.* **82**(3) 2731–2784
- [8] Kalashnikova A M, Kimel A V and Pisarev R V 2015 *Phys. Usp.* **58** 969–980
- [9] Baranov P G *et al.* 2019 *Phys. Usp.* **62** 795–822
- [10] Satoh T, Terui Y, Moriya R, Ivanov B A, Ando K, Saitoh E, Shimura T and Kuroda K 2012 *Nature Photonics* **6** 662–666
- [11] Au Y, Dvornik M, Davison T, Ahmad E, Keatley P S, Vansteenkiste A, Van Waeyenberge B and Kruglyak V V 2013 *Phys. Rev. Lett.* **110**(9) 097201
- [12] Parkes D E *et al.* 2013 *Scientific reports* **3** 2220
- [13] Khokhlov N E, Gerevenkov P I, Shelukhin L A, Azovtsev A V, Pertsev N A, Wang M, Rushforth A W, Scherbakov A V and Kalashnikova A M 2019 *Physical Review Applied* **12** 044044
- [14] Krebs J J, Jonker B T and Prinz G A 1987 *Journal of Applied Physics* **61** 2596–2599
- [15] Damon R W and Eshbach J R 1961 *Journal of Physics and Chemistry of Solids* **19** 308–320
- [16] Kalyabin D V, Sadovnikov A V, Beginin E N and Nikitov S A 2019 *Journal of Applied Physics* **126** 173907
- [17] Kamimaki A, Iihama S, Sasaki Y, Ando Y and Mizukami S 2017 *Phys. Rev. B* **96**(1) 014438
- [18] Kamimaki A, Iihama S, Sasaki Y, Ando Y and Mizukami S 2017 *IEEE Transactions on Magnetics* **53** 1–4
- [19] Kolokoltsev O, Qureshi N, Mejía-Uriarte E and Ordóñez-Romero C L 2012 *Journal of Applied Physics* **112** 013902
- [20] Grundler D 2015 *Nature Physics* **11** 438–441